

Radiolabelling of 1,4-disubstituted 3-[¹⁸F]fluoropiperidines and its application to new radiotracers for NR2B NMDA receptor visualization†Radouane Koudih,^{‡,a,b,c} Gwénaëlle Gilbert,^{‡,a,b,c} Martine Dhilly,^{a,b,c} Ahmed Abbas,^d Louisa Barré,^{a,b,c} Danièle Debruyne^{a,b,c} and Franck Sobrio^{*a,b,c}

Received 17th July 2012, Accepted 5th September 2012

DOI: 10.1039/c2ob26378e

In order to develop a novel and useful building block for the development of radiotracers for positron emission tomography (PET), we studied the radiolabelling of 1,4-disubstituted 3-[¹⁸F]fluoropiperidines. Indeed, 3-fluoropiperidine became a useful building block in medicinal chemistry for the pharmacomodulation of piperidine-containing compounds. The radiofluorination was studied on substituted piperidines with electron-donating and electron-withdrawing *N*-substituents. In the instance of electron-donating *N*-substituents such as benzyl or butyl, configuration retention and satisfactory fluoride-18 incorporation yields up to 80% were observed. In the case of electron-withdrawing *N*-substituents leading to carbamate or amide functions, the incorporation yields depend on the 4-substituent (2 to 63%). The radiolabelling of this building block was applied to the automated radiosynthesis of NR2B NMDA receptor antagonists and effected by a commercially available radiochemistry module. The *in vivo* evaluation of three radiotracers demonstrated minimal brain uptakes incompatible with the imaging of NR2B NMDA receptors in the living brain. Nevertheless, moderate radiometabolism was observed and, in particular, no radiodefluorination was observed which demonstrates the stability of the 3-position of the fluorine-18 atom. In conclusion, the 1,4-disubstituted 3-[¹⁸F]fluoropiperidine moiety could be of value in the development of other radiotracers for PET even if the evaluation of the NR2B NMDA receptor antagonists failed to demonstrate satisfactory properties for PET imaging of this receptor.

Introduction

Piperidines are widely present in natural bioactive substances and are also used in medicinal chemistry which has led to numerous original drugs. In structure–activity relationship studies, the piperidine is mainly employed either as an *N*-substituted aliphatic amine or substituted in the 4-position. Among various modifications of the piperidine pharmacophore, the 3-fluoropiperidine moiety is present in some bioactive compounds such as Y1 neuropeptide Y receptor antagonists^{1,2} and M1 muscarinic receptor agonists³ and has led, in some

cases, to improved pharmacological properties⁴ with, as examples, serotonergic 5-HT_{1D} receptor ligands,⁵ T-type calcium channel inhibitor **1**,^{6–9} PAR1 protease activated receptor antagonist **2**,¹⁰ kinesin spindle protein KSP inhibitors⁸ and NR2B NMDA antagonist **3**¹¹ (Chart 1).

Positron emission tomography (PET) is an imaging technique used for diagnosis and prognosis, and to explore the disease states as well as to validate innovative therapies or drugs. The development of this non-invasive technique and its extensive clinical use are due to the availability of commercial radiopharmaceuticals labelled with fluorine-18. The weak energy of the emitted positron affords high resolution images. The production capacities in quantity of fluoride-18 as well as a half-life of 109.7 min are compatible with transportation and in consequence fluorine-18 became the radioisotope of choice for PE. The development of this radiofluorinated family of radiotracers is linked to the increased number of fluorinated building blocks and radiolabelling methods.^{12,13}

To enrich the number of radiofluorinated building blocks, we studied the radiolabelling of different *N*-substituents containing 4-substituted-3-fluoro-piperidines. To evaluate the usefulness of this radiofluorinated moiety, we labelled NR2B subunit containing *N*-methyl-D-aspartate receptor (NMDAR) antagonists.

^aCEA, I2BM, LDM-TEP, UMR 6302 ISTCT, GIP Cyceron, BP5229 F-14074 Caen, France. E-mail: sobrio@cyceron.fr;

Fax: +33 2 3147 0225; Tel: +33 2 3147 0264

^bUniversité de Caen Basse-Normandie, UMR 6302 ISTCT, LDM-TEP, GIP Cyceron, F-14074 Caen, France

^cCNRS, UMR 6302 ISTCT, LDM-TEP, GIP Cyceron, F-14074 Caen, France

^dINSERM U1077, GIP Cyceron, F-14074 Caen, France

†Electronic supplementary information (ESI) available: Synthetic procedures for **3–32**, *in silico* pharmacological properties and NMR spectra for **4**, **5**, **6**, **7**, **8**, **9**, **10**, **11**, **12**, **18**, **19**, **20**, **21** and **29**. See DOI: 10.1039/c2ob26378e

‡These authors had equally contributed to this work.

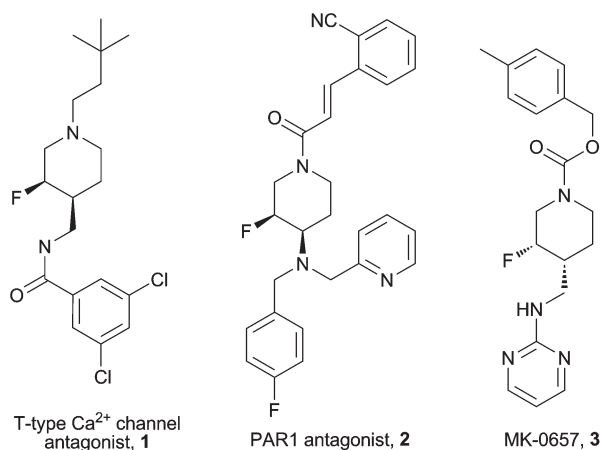


Chart 1 Structure of 3-fluoropiperidines containing bioactive compounds.

NMDARs are heteromeric complexes of NR1 and NR2 subunits that mediate rapid excitatory neurotransmission throughout the central nervous system (CNS). NR2 subunits result from four distinct genes that construct NR2A–D subunits that have diverse pharmacological properties and substantially different expression patterns in the brain.¹⁴ The NR2B subunit containing NMDARs is the focus of increasing interest as a therapeutic target¹⁵ in many of CNS pathologies, including stroke, acute and chronic pain, drug-induced dyskinesia and dementia.^{16,17} The radiotracers to study the NMDARs are the subject of intensive studies but none so far have been suitable for clinical or even preclinical imaging.^{18–20} Recently, we reported the radiosynthesis of two radiotracers, [¹⁸F]MK-0567 ([¹⁸F]*cis*-**3**) and its *trans*-isomer, [¹⁸F]*trans*-**3**.²¹ Their *in vitro* evaluation based on the autoradiography of the rat brain demonstrated high specific binding for NR2B subunit containing NMDARs located in rich NR2B regions. The K_d was 9.1 ± 2.1 nM and 7.1 ± 1.7 nM in the hippocampus for [¹⁸F]MK-0567 and its *trans*-[¹⁸F]isomer, respectively. The K_d/B_{max} ratios for both radiotracers varied from 17 to 37 as a function of the anatomical localization as well as the log $D_{7.4}$ (2.66 and 2.80 for [¹⁸F]*trans*-**3** and [¹⁸F]*cis*-**3**, respectively) indicates favourable properties for the CNS imaging of the NR2B NMDARs.

Herein we report the radiolabelling of 4-trityloxymethyl-3-[¹⁸F]fluoropiperidine model compounds that contain different *N*-substituents, their application to the radiosynthesis of radiofluorinated NR2B NMDAR antagonists and their *in vivo* evaluation in μ PET imaging studies.

Results and discussion

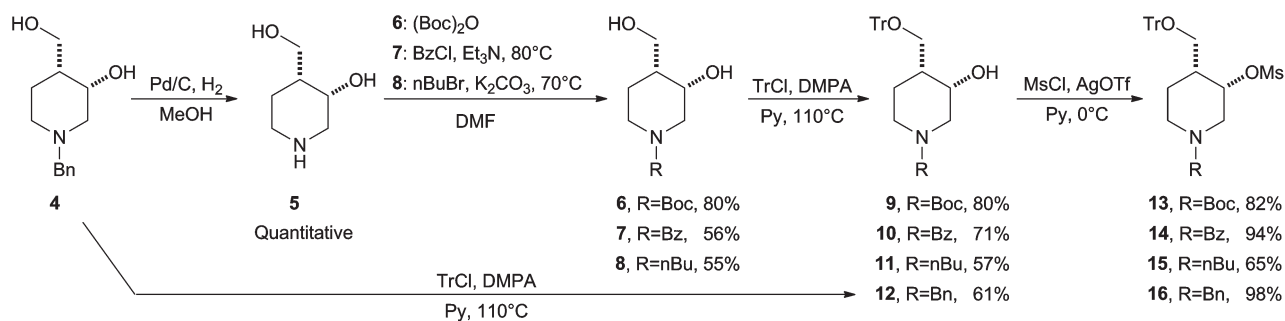
Chemistry

The radiofluorination of 3-[¹⁸F]fluoropiperidines was envisaged based on the mesylate leaving group which could be obtained from the corresponding alcohol. The 4-hydroxymethylpiperidiny moiety was chosen because piperidin-3-ol (**4**) was previously described^{22,23} and the corresponding 3-fluoropiperidine (**17**) was synthesized by DiFabio and coll.¹ Butyl and benzyl were chosen as electron-donating groups given their presence in many

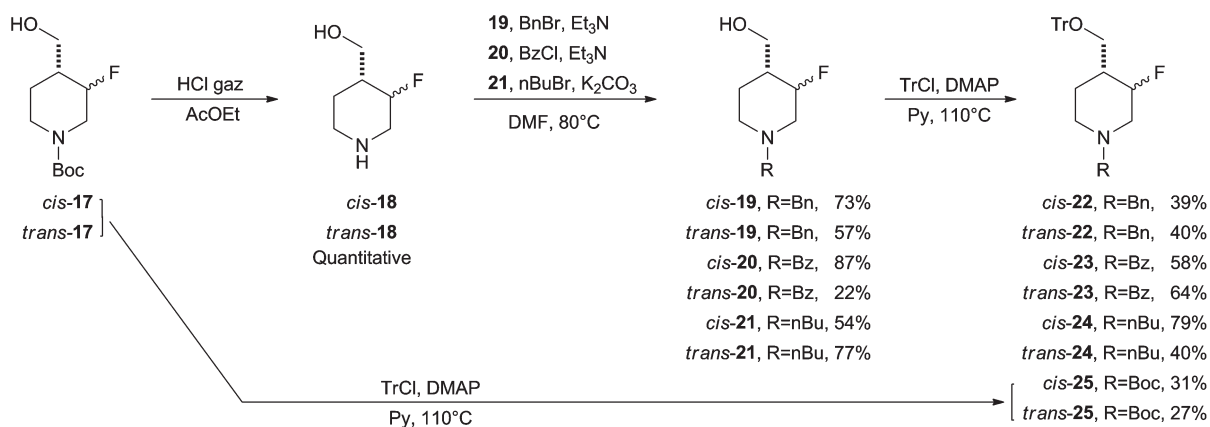
bioactive compounds.^{5–7} As carbamate and amide functions are found in several ligands,^{10,21} the benzoyl and *tert*-butyl carboxylate were selected as electron-withdrawing groups to study the radiofluorination reaction. The addition of a trityl group could be selectively performed on the primary alcohol. Then the secondary alcohol could react with mesyl chloride to form the mesylate precursor. The presence of the trityl chromophore group allowed the ready detection of the compound in HPLC. Thereafter, the labelling precursors **13–16** with the *cis*-configuration were prepared (Scheme 1) from the *N*-benzyl diol **4** by the removal of the *N*-benzyl group followed by reaction with the corresponding alkyl or benzoyl halide. After selective O-alkylation with trityl chloride of the primary alcohol, the mesylation was achieved with mesylate chloride in the presence of silver triflate in pyridine²⁴ to give the labelling precursors **13–16**. The preparation of the fluorinated *O*-trityl compounds (**22–25**) was performed after deprotection of the Boc group following the same synthetic pathway (Scheme 2). Addition of the trityl group created the fluorinated *cis* and *trans* isomers **22–25** needed for the identification of the radiolabelled compounds by co-migration in HPLC. To further explore the scope and applications of radiofluorination reaction, the *N*-Boc-4-(pyrimidin-2-yl)aminomethyl-3-mesyloxy-piperidine precursor *cis*-**31** was obtained from the 3-hydroxy analogue²¹ by mesylation (Scheme 3). The preparation of the fluorinated reference compound **32** as well as the synthesis of NR2B NMDAR antagonists *cis*- and *trans*-**3** and their radiolabelling precursors *cis*-**30** and *trans*-**30** have been described previously (Scheme 3).²¹ Amide coupling of *trans*-2-phenylcyclopropane-1-carboxylic acid and the piperidine obtained from the removal of the Boc group of *trans*-**32** gave *trans*-**33**. The labelling precursor *cis*-**29** was prepared following the same methodology (Scheme 3).

Radiolabelling

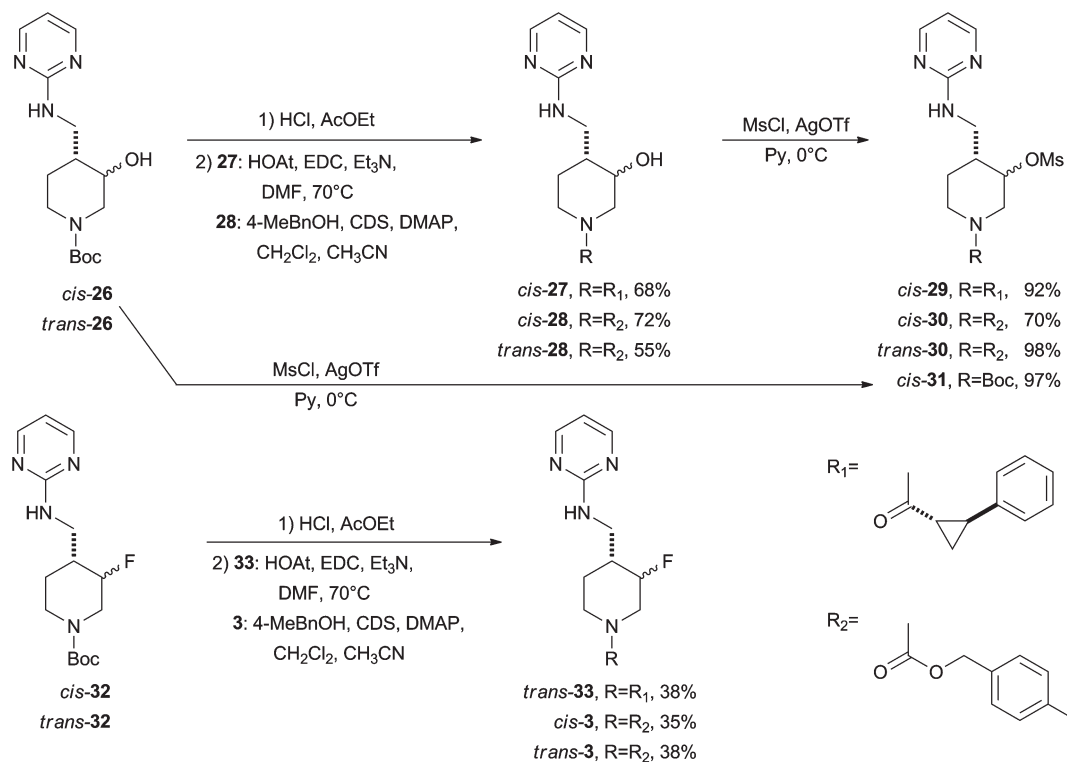
The radiolabelling was performed under classical nucleophilic radiofluorination conditions based on the complex [$K^{18}F/K_{2.2.2}$] as the source of reactive “naked” fluoride (Scheme 4). In brief, [¹⁸F]fluoride, produced by the ¹⁸O(p,n)¹⁸F nuclear reaction, was trapped in a quaternary ammonium resin solid phase extraction (SPE) cartridge. The [¹⁸F]fluoride was eluted by a potassium carbonate solution and dried in the presence of Kryptofix 2.2.2 ($K_{2.2.2}$) by successive azeotropic evaporation with acetonitrile. The amount of the complex and the solvent of reaction as well as the reaction temperature were varied (Table 1). The incorporation yield of fluorine-18 into compounds [¹⁸F]**22–25**, [¹⁸F]**32–33** and [¹⁸F]**3** was established by radioTLC and the identity of the radiolabelled product was established by co-migration on HPLC with the non-radioactive reference compound. For each compound, the two diastereoisomers were prepared and separated by HPLC (Table 2). The kinetics of the reaction were studied over 20 min which was the reaction time leading to a high incorporation yield with low variability. The radiofluorination of the *cis*-mesyloxy *N*-butyl and *N*-benzyl precursors (**15** and **16**) was performed with moderate to excellent yields (entries 1–4) of the *cis* products, [¹⁸F]*cis*-**24** and [¹⁸F]*cis*-**22** respectively. The conservation of the configuration resulted from a double S_N2 substitution also called neighbouring-group participation,



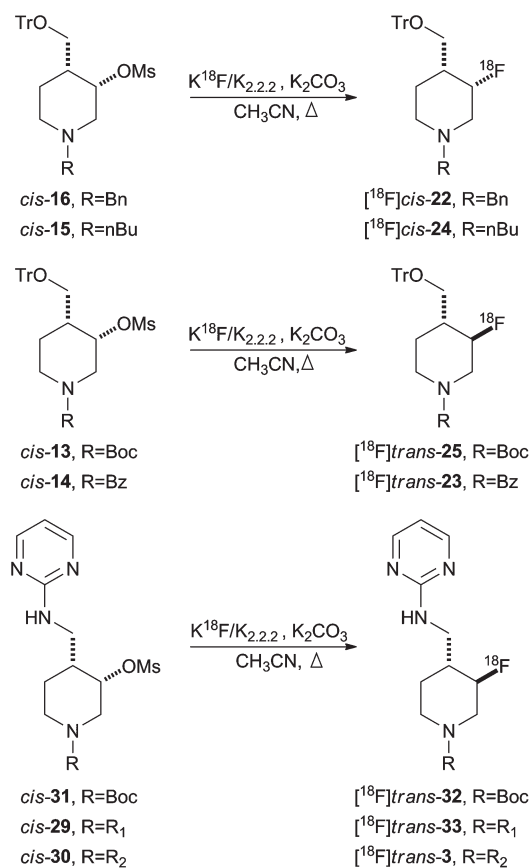
Scheme 1 Synthesis of labelling precursors 13–16.



Scheme 2 Synthesis of reference compounds 22–25.



Scheme 3 Synthesis of NR2B NMDAR antagonists 3 and 33 and their radiolabelling precursors.



Scheme 4 Radiofluorination reactions.

which proceeds by an aziridinium intermediate (Scheme 5),²⁵ the formation of which was due to the availability of the electronic doublet of the nitrogen atom in the piperidine²⁵ enriched by the electron-donating substituents. The selective opening of the aziridinium ring by the [¹⁸F]fluoride occurred on the more hindered atom (Scheme 4).²⁶ In the case of an electron-withdrawing substituent on piperidine like carboxylate or carbonyl, the inversion of conformation indicated an S_N2 mechanism (entries 5–21). With methoxytrityl in the 4-position and *N*-Boc or *N*-benzoyl substituents (**13** and **14**), the radiofluorination gave the [¹⁸F]*trans*-**25** and [¹⁸F]*trans*-**23** in very low yields (entries 5–12). Further, we studied the scope of the reaction and excluded a steric effect of the trityl group which could explain the poor incorporation rate for the compounds **13** and **14**, by the reaction with the 4-(pyrimidin-2-ylamino)methyl substituted piperidine **31**.²¹ The fluorine-18 incorporation was effected in acetonitrile with a good yield (entry 13). No effect other than a steric one was proposed for the difference of incorporation yields between pyrimidin-2-ylamino and trityloxy substituted compounds [¹⁸F]*trans*-**25** and [¹⁸F]*trans*-**32**. For the radiolabelling of [¹⁸F]*trans*-**32**, a reaction temperature of 80 °C led to a 19–27% incorporation yield and could be improved to 32–47% at 95 °C (entries 14 and 16). The use of DMSO at 120 °C did not improve the labelling rate (entries 8, 15, 12 and 21). The radiofluorinations of the NR2B antagonists, *cis*-**3** and *trans*-**3**, were performed under the same conditions as those of the *N*-Boc-piperidine **31** since the *N*-substituent was also a carbamate. The incorporation yield

was less (40% vs. 62%) but identical for the both diastereoisomers (entries 17–18). The radiolabelling of the *N*-carbonyl compound, [¹⁸F]*trans*-**33**, was obtained with an incorporation yield of fluorine-18 around 26% (entry 19). When the standard quantity of the [K¹⁸F/K_{2.2.2}] complex was employed (entries 2, 4, 6, 10, 14, 16 and 20), the radiochemical yields were significantly lower than when a reduced amount of complex was used. These poor yields could be due to the competing elimination reaction which was shown by the characterization of the alkene resulting from the elimination reaction with **31**. In this case, the percentage of the elimination product was about 60% of the precursor *versus* 23% under the most optimal conditions (entry 13).

Radiotracer radiosyntheses

Recently, we described the radiosyntheses of the radiotracers [¹⁸F]*cis*-**3**, [¹⁸F]*trans*-**3** through the use of a widely available commercial TRACERlab FX-FN module (GE Healthcare).²¹ The same conditions were used for the preparation of [¹⁸F]*trans*-**33**. After azeotropic drying, the [K¹⁸F/K_{2.2.2}] complex was reacted with the precursor *cis*-**30**, *trans*-**30** or **29** (10 μmol respectively) in acetonitrile (1 mL) at 90 °C for 20 min. After dilution with water, the prepurification was achieved through a C18 SPE cartridge. The radioactive product was eluted from the cartridge by acetonitrile and purified by reversed phase HPLC. The pure fraction containing the [¹⁸F]-product was collected and submitted to a reformulation by SPE to obtain a radioactive concentrated saline solution for i.v. injection containing less than 10% of ethanol. The data concerning the radiosynthesis are described in Table 3. 400 to 750 MBq of the radiolabelled product were obtained with acceptable and reliable radiochemical yields after reformulation. High specific radioactivities were measured between 170 to 590 GBq μmol⁻¹ and the radiochemical purities of the radiotracers were established by HPLC and were greater than 98%.

In vivo pharmacological evaluation of the radiotracers

Compound *cis*-**3** (MK-0657) was developed by Merck laboratories²⁷ and clinical trials were conducted to evaluate its effects in the treatment of major depression and in the motor function improvement in Parkinson's disease patients.²⁸ Our recent *in vitro* findings on [¹⁸F]*cis*-**3** and [¹⁸F]*trans*-**3** warrant the *in vivo* evaluation of these radiotracers.²¹ In the same patent describing *cis*- and *trans*-**3**,²⁷ several antagonists presenting similar activity were described among them, an amide (**33**) caught our attention due to the *in silico* predicted properties of this compound[§] and to the presence of the amide function which could validate our radiolabelling strategy. The radiotracers (16 ± 5 MBq) were administered to rats and were evaluated by μPET and *ex vivo* measurements. The brain uptake kinetics were determined by reconstruction of PET time activity curves from 0 to 90 min. The radioactivity peaked by 1 min post-injection; thereafter, all three radiotracers were rapidly cleared from the brain (Fig. 1). At 90 min, the brain/blood ratios were 1.97 ([¹⁸F]*trans*-**3**) and 1.88 ([¹⁸F]*cis*-**3**) and the brain showed a poor contrast corresponding

§ See ESI for the *in silico* predicted pharmacological properties.

Table 1 Summary of ^{18}F labelling reaction

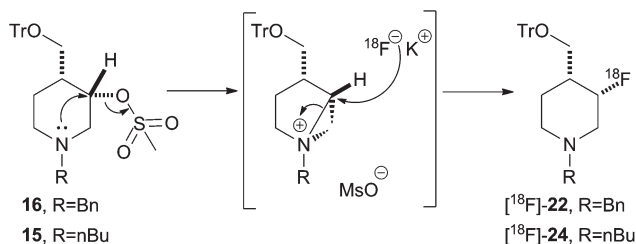
Reaction entry	Precursor	$\text{K}_{222}/\text{K}_2\text{CO}_3$ (mg)	Solvent	Reaction temperature ^a	^{18}F -product	^{18}F incorporation yield ^b (%)
1	<i>cis</i> -15	6.8/2.1	Acetonitrile	90 °C	^{18}F <i>cis</i> -24	78–81%
2	<i>cis</i> -15	22/7	Acetonitrile	90 °C	^{18}F <i>cis</i> -24	48–55%
3	<i>cis</i> -16	6.8/2.1	Acetonitrile	90 °C	^{18}F <i>cis</i> -22	29–37%
4	<i>cis</i> -16	22/7	Acetonitrile	90 °C	^{18}F <i>cis</i> -22	10–14%
5	<i>cis</i> -13	6.8/2.1	Acetonitrile	90 °C	^{18}F <i>trans</i> -25	2–5%
6	<i>cis</i> -13	22/7	Acetonitrile	90 °C	^{18}F <i>trans</i> -25	<2%
7	<i>cis</i> -13	6.8/2.1	DMF	100 °C	^{18}F <i>trans</i> -25	1–3%
8	<i>cis</i> -13	6.8/2.1	DMSO	100 °C	^{18}F <i>trans</i> -25	4–6%
9	<i>cis</i> -14	6.8/2.1	Acetonitrile	90 °C	^{18}F <i>trans</i> -23	2–4%
10	<i>cis</i> -14	22/7	Acetonitrile	90 °C	^{18}F <i>trans</i> -23	<2%
11	<i>cis</i> -14	6.8/2.1	DMF	100 °C	^{18}F <i>trans</i> -23	2–4%
12	<i>cis</i> -14	6.8/2.1	DMSO	100 °C	^{18}F <i>trans</i> -23	<2%
13	<i>cis</i> -31	6.8/2.1	Acetonitrile	95 °C	^{18}F <i>trans</i> -32	60–65%
14	<i>cis</i> -31	22/7	Acetonitrile	95 °C	^{18}F <i>trans</i> -32	32–47%
15	<i>cis</i> -31	6.8/2.1	DMSO	120 °C	^{18}F <i>trans</i> -32	63–64%
16	<i>cis</i> -31	22/7	Acetonitrile	80 °C	^{18}F <i>trans</i> -32	19–27%
17	<i>cis</i> -30	6.8/2.1	Acetonitrile	95 °C	^{18}F <i>trans</i> -3	33–42%
18	<i>trans</i> -30	6.8/2.1	Acetonitrile	95 °C	^{18}F <i>cis</i> -3	31–45%
19	<i>cis</i> -29	6.8/2.1	Acetonitrile	95 °C	^{18}F <i>trans</i> -33	25–27%
20	<i>cis</i> -29	22/7	Acetonitrile	95 °C	—	None
21	<i>cis</i> -29	6.8/2.1	DMSO	120 °C	^{18}F <i>trans</i> -33	23–38%

^a Reaction conditions: precursor, 10 μmol ; solvent, 1 mL; reaction time, 20 min. ^b Incorporation yields were determined by radio-TLC. $n \geq 3$ experiments.

Table 2 HPLC conditions used for the identification of the radiolabelled products

Retention time (min)			HPLC conditions ^a $\text{H}_2\text{O}/\text{CH}_3\text{CN}/\text{TFA}$ (v : v : v)	
Precursor	<i>Cis</i> -product	<i>Trans</i> -product		
9.5	(<i>cis</i> -13)	15.1 (<i>cis</i> -25)	18.7 (<i>trans</i> -25)	80/20 ^b
5.9	(<i>cis</i> -14)	9.7 (<i>cis</i> -23)	8.5 (<i>trans</i> -23)	80/20 ^b
10.8	(<i>cis</i> -15)	14.8 (<i>cis</i> -24)	16.9 (<i>trans</i> -24)	50/50/0.1 ^b
12.4	(<i>cis</i> -16)	10.3 (<i>cis</i> -22)	11.5 (<i>trans</i> -22)	50/50/0.1 ^b
9.9	(<i>cis</i> -29)		12.5 (<i>trans</i> -33)	55/45 ^b
10.1	(<i>cis</i> -30)	12.5 (<i>cis</i> -3)	14.6 (<i>trans</i> -3)	55/45 ^c
19.7	(<i>trans</i> -30)	18.6 (<i>cis</i> -3)	23.7 (<i>trans</i> -3)	60/40 ^c
8.2	(<i>cis</i> -31)	9.3 (<i>cis</i> -32)	12.1 (<i>trans</i> -32)	40/60 ^c

^a Conditions: flow: 1 mL min^{-1} , UV detection: 234 nm. ^b Column Nucleodur C18 Isis (Macherey-Nagel), 250 \times 4 mm, 5 μm . ^c Column Nucleodur C18 Pyramid (Macherey-Nagel), 250 \times 4 mm, 5 μm .

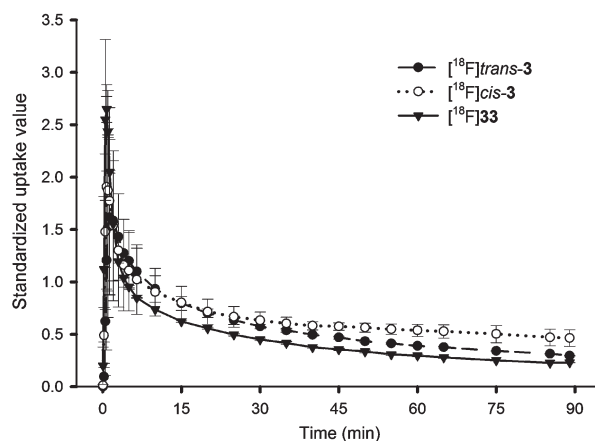
**Scheme 5** Radiolabelling mechanism for ^{18}F -22 and ^{18}F -24.

to an uptake index (UI) lower than 1 (Fig. 2). Only a slight difference of brain uptake was observed with a UI = 0.55 for ^{18}F *cis*-3 related to UI = 0.39 for ^{18}F *trans*-3. The brain/blood ratio for ^{18}F 33 was evaluated to be 0.35 with a very low UI =

Table 3 Summary of the radiotracer syntheses

^{18}F product	Radiochemical yield ^a	Specific radioactivity ^b (GBq μmol^{-1})	Radiosynthesis time
^{18}F <i>cis</i> -3	13 \pm 5%	170 \pm 80	100 min
^{18}F <i>trans</i> -3	18 \pm 6%	326 \pm 45	89 min
^{18}F <i>trans</i> -33	9 \pm 1%	592 \pm 150	123 min

^a Relative to ^{18}F -fluoride and decay corrected to the end of bombardment. ^b At the end of synthesis.

**Fig. 1** μPET radioactivity kinetics in rat brain of the radiotracers ($n = 3$).

0.14 which could be due to a lower stock level in fat. No significant differences were observed between the accumulations of radioactivity within the different brain structures (Fig. 3). The target to non-target ratio, such as the cortex to cerebellum ratio,

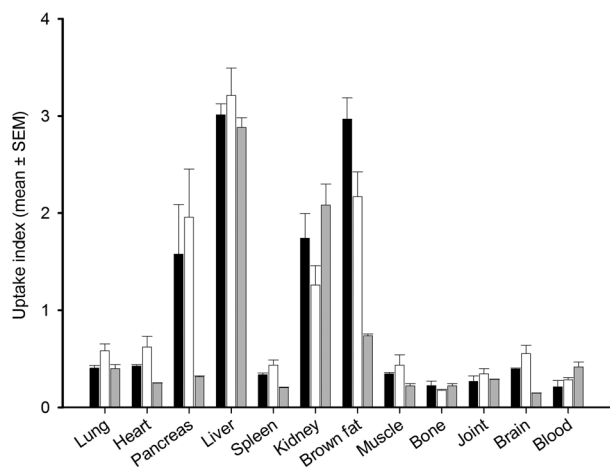


Fig. 2 *Ex vivo* organ and tissue distribution in rat at 90 min post-injection: black bars, $[^{18}\text{F}]trans\text{-}3$; white bars, $[^{18}\text{F}]cis\text{-}3$; grey bars, $[^{18}\text{F}]33$ ($n = 3$).

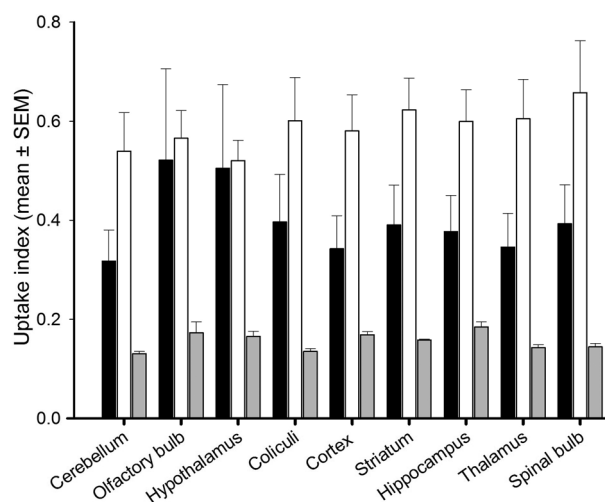


Fig. 3 *Ex vivo* cerebral distribution in rat brain at 90 min post-injection: black bars, $[^{18}\text{F}]trans\text{-}3$; white bars, $[^{18}\text{F}]cis\text{-}3$; grey bars, $[^{18}\text{F}]33$ ($n = 3$).

was essentially unit and thus in disagreement with the heterogeneity observed *in vitro*.²¹ In addition, the simultaneous administration of a non-radioactive compound did not significantly affect the regional cerebral uptakes which would imply a high non-specific binding of these radioligands *in vivo*. The *in vivo* metabolism of $[^{18}\text{F}]3$ and $[^{18}\text{F}]33$ was investigated over time by μPET scanning in the anesthetized rat. Radiometabolite analysis indicated that parent tracers were still prevalent at 45 min (Fig. 4). The terminal half-life of the parent compound, $[^{18}\text{F}]trans\text{-}3$, $[^{18}\text{F}]cis\text{-}3$ and $[^{18}\text{F}]33$, was 58 min, 53 min and 22 min respectively. In the rat brain, about 79% ($[^{18}\text{F}]trans\text{-}3$), 71% ($[^{18}\text{F}]cis\text{-}3$) and only 51% ($[^{18}\text{F}]33$) of the initial compound remained unchanged at 90 min. In tissue dissection studies, the highest radioactivity concentrations at 90 min post-injection were measured in the liver and brown fat, followed by the pancreas and kidney while the lowest levels were in the blood and bones for $[^{18}\text{F}]trans\text{-}3$ and $[^{18}\text{F}]cis\text{-}3$. The peripheral tissue distribution

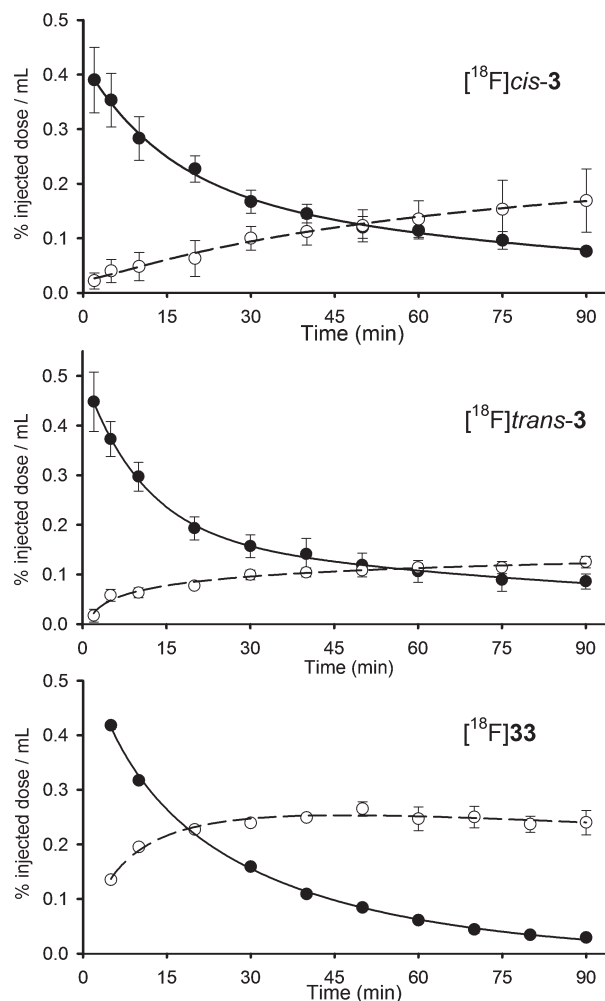


Fig. 4 Radioactive plasmatic kinetics of the radiotracers in rat: closed circle and plain line, $[^{18}\text{F}]$ -parent compound; open circle and dashed line, polar $[^{18}\text{F}]$ -radiometabolites ($n = 3$).

of $[^{18}\text{F}]33$ differed with a lower uptake in brown fat and pancreas (Fig. 2). The accumulation of activity in the bone was low with bone/blood radioactivity concentration ratios of 1.05, 0.62 and 0.52 for $[^{18}\text{F}]trans\text{-}3$, $[^{18}\text{F}]cis\text{-}3$ and $[^{18}\text{F}]33$ respectively, at 90 min post-injection (Fig. 2). The absence of accumulation in bones and joints demonstrated the stability of the $[^{18}\text{F}]$ -3-fluoropiperidine moiety *versus* radiodefluorination. The high uptake in fatty tissues at 90 min points towards a lipophilicity such that the capacity of both $[^{18}\text{F}]3$ radiotracers to image the brain is questionable in spite of a $\log D_{7.4}$ less than 2.8 (2.80 ± 0.02 and 2.66 ± 0.09 for $[^{18}\text{F}]cis\text{-}3$ and $[^{18}\text{F}]trans\text{-}3$ respectively). The lower fat uptake for $[^{18}\text{F}]33$ could be correlated to its lower $\log D_{7.4}$ (2.36 ± 0.09).

Experimental

Chemistry

The material and reagents part as well as the synthetic procedures are given in the ESI.†

Radiochemistry

Radioisotope production. No-carrier-added aqueous [^{18}F] fluoride was produced by the $^{18}\text{O}[\text{p,n}]^{18}\text{F}$ nuclear reaction of a target consisting of ^{18}O -enriched water (97%, Eurisotop) irradiated with a 18 MeV proton beam (IBA Cyclone 18/9 cyclotron).

Preparation of nucleophilic [^{18}F]fluoride ion. [^{18}F] F^- was separated from ^{18}O -enriched water using an ion exchange resin (QMA light, Waters, ABX) eluted with aqueous potassium carbonate (5 mg mL $^{-1}$, 300 μL). The [^{18}F]fluoride solution was collected into a conical reactivial® containing Kryptofix 2.2.2 (22 or 6.8 mg) and K_2CO_3 (adjusted to obtain 7 or 2.1 mg) dissolved in a water–acetonitrile mixture (600 μL , 1 : 1, v : v). The water was removed azeotropically with acetonitrile (2 \times 600 μL) under a stream of nitrogen at 110 $^\circ\text{C}$, affording a dry residue of [K/K_{222}] $^{+18}\text{F}^-$. Between 1 mCi (37 MBq) and 5 mCi (185 MBq) of dried [K/K_{222}] $^{+18}\text{F}^-$ were obtained in 20 min.

Radiofluorination reaction. A solution of the labelling precursor (10 μmol) dissolved in either DMSO, MeCN or DMF (1 mL) was added to the dried [K/K_{222}] $^{+18}\text{F}^-$ complex and the sealed reaction vial was heated (45–120 $^\circ\text{C}$) for 20 min. Aliquots (25 μL) were taken at 5, 10 and 20 min and were subjected to radioTLC and/or radioHPLC analysis after dilution with an HPLC mobile phase. The radiochemical yield was determined from radioTLC representing the percentage of radioactivity area of the labelled product related to the total radioactivity area. TLC elution conditions for all compounds were CH_2Cl_2 –MeOH; 95 : 5.

Radiosynthesis of radiotracers [^{18}F]-3 and [^{18}F]-33 with GE TRACERLab FX $_{\text{FN}}$. The fluorine-18 produced by the cyclotron was trapped on an ion exchange resin (QMA light, Waters, ABX), separated from ^{18}O -enriched water then eluted with a solution of potassium carbonate and Kryptofix 2.2.2 in acetonitrile (0.3 mL) and water (0.3 mL) (vial 1). The mixture was heated to 95 $^\circ\text{C}$ under reduced pressure under a flow of helium. 0.6 mL of acetonitrile (vial 2) was added and the mixture was further heated at 95 $^\circ\text{C}$ under reduced pressure. About 5 mg (10 μmol) of the labelling precursor **30** or **29** in 1 mL of acetonitrile (vial 3) was added to the reactor and the reaction mixture was heated at 95 $^\circ\text{C}$ for 20 min, then diluted with 2 mL of water (vial 4). The reaction mixture was passed through an SPE cartridge (Shorty C18 ec, 20 mg, Macherey-Nagel) to separate the radio-labeled product from the reaction mixture. The cartridge was eluted with 0.5 mL of acetonitrile (vial 5) then washed with 0.5 mL of water (vial 6). 200 μL of this elution solution was injected into an HPLC column to facilitate the separation (column: Nucleosil 100-5 C-18 Nautilus, 250 \times 10 mm, Macherey-Nagel; eluent: acetonitrile– H_2O , 35 : 65 for t_{R} (*cis*-**3**) = 36 min and 37 : 63 for t_{R} (*trans*-**3**) = 38 min; eluent: acetonitrile– H_2O , 27 : 73 for t_{R} (*trans*-**33**) = 57 min flow rate: 6 mL min $^{-1}$). The collected fraction containing the pure radiolabeled product was diluted with 25 to 40 mL of water and then passed through an SPE cartridge (Shorty C18 ec, Macherey-Nagel). The cartridge was then washed with 2 mL of water (vial 9) and eluted with 0.2 mL of ethanol (vial 8) and 1.8 mL of saline (vial 7).

The radiochemical purity of the radiotracers was determined by HPLC following the conditions described in Table 2 and was more than 98%. The specific radioactivity was measured by the radioactivity concentration/molar concentration obtained by UV absorption in HPLC and calibration curves established from the reference compounds ratio.

Pharmacological evaluation

μPET imaging. The animal experiments were conducted according to the appropriate European Directives (86/609/EEC) and French National Legislation and in conformity with the Guiding Principles in the Care and Use of Animals as approved by the University of Caen. Male Sprague–Dawley rats (250–310 g, C.E.R.J., France) were induced with isoflurane 5% and maintained under anesthesia with isoflurane 1.5–2.5% in oxygen and nitrous oxide (30/70) for the duration of the experiment. Rats were positioned in an Inveon® μPET (Siemens, Saint Denis, France) with brain centred in the field of view. A transmission scan of 10 min using a cobalt-57 source was performed before tracer injection to provide attenuation correction. [^{18}F]*trans*-**3** or [^{18}F]*cis*-**3** were injected (16.6 \pm 5.5 MBq) *via* a catheter in the tail vein to animals ($n = 3$). For co-administration studies, non-radioactive reference compounds (*trans*-**3** or *cis*-**3**, 30 μg , 84 μmol *i.e.* about 1000-fold the injected radiotracer amount) were injected simultaneously with the radiotracer. PET dynamic images were reconstructed from 0 to 30 or 90 min emission scans with an OSEM 2D algorithm using the Inveon Acquisition Workplace Software (Siemens Medical solution, Knoxville, USA). An analytical scatter correction was implemented for the image reconstruction. Decay corrected time–activity curves (TAC) were obtained for the regions of interest (ROI) selected in the upper part of the rat body: brain, wrist articulation, liver and cervical brown adipose tissue. Radioactivity data were injected dose- and bodyweight-normalized by expression of SUV (Standardized Uptake Value).

***Ex vivo* biodistribution.** During the μPET examination, successive blood samples were taken off from the femoral artery from 0 to 90 min and were immediately centrifuged. Plasma samples (5 μL) were placed in the γ -counter Packard Cobra for measuring the radioactivity. Rats were killed under anesthesia at the end of the μPET exam. Organs and tissues (heart, liver, lung, kidney, spleen, skeletal muscle, bone, joint, brown fat and pancreas) were collected, blotted, weighed and counted. The brain was carefully removed, blotted and cut into two parts according to the sagittal way. Half of the brain was weighed and counted and the other half was dissected into cerebellum, hypothalamus, colliculi, cortex, striatum, hippocampus and thalamus. Radioactivity in each tissue or plasma sample was measured with a γ -counter Packard Cobra (Perkin Elmer, Courtaboeuf, France) and corrected for decay. Radioactivity data were injected dose- and bodyweight-normalized by expression of UI (Uptake Index).

***In vivo* radiometabolism study.** For radiometabolite analyses of plasma, acetonitrile was added to plasma (1/1: v/v), vortexed and centrifuged. The supernatant was analysed by radioTLC using a silica-gel TLC (Merck) and CH_2Cl_2 –MeOH (95 : 5) as a mobile phase. To assess the radiometabolism of [^{18}F]*trans*-**3** or

[^{18}F]cis-3 in the rat brain, rats were killed at 30 min after radiotracer injection. The whole brains were rapidly removed, homogenized in acetonitrile and centrifuged and the supernatant was analysed by HPLC (eluent: H_2O – MeCN ; 60 : 40). The percentage of unchanged [^{18}F]trans-3 or [^{18}F]cis-3 with respect to total plasma radioactivity was obtained by measuring counts related to parent radiotracer and radiometabolites from each time point. The identification of the parent compound was achieved on the sample at the latest time after administration by radioHPLC (eluent: H_2O – MeCN ; 60 : 40) and comigration with the non-radioactive reference.

Conclusions

We have demonstrated that the ^{18}F -labelled 3-fluoro-4,1-substituted-piperidine could be obtained with a good yield with variation of both the 4-position substituent and the *N*-substituent. In the case of an alkyl or benzyl substituent on the piperidine (*i.e.* electron-donating groups), the incorporation yield was excellent via a double $\text{S}_{\text{N}}2$ mechanism which conserves the configuration. When the *N*-substituents were carbonyl or carboxylate (*i.e.* electron-withdrawing substituents), the incorporation of fluorine-18 depended on the 4-substituent and each time inverted the configuration. We applied the labelling of this moiety, with success, to the radiosynthesis of three antagonists of the NR2B subunit-containing NMDA receptor. The radiotracers labelled with fluorine-18 by a one-step nucleophilic substitution reaction were efficiently and reliably produced with high specific radioactivity. Despite promising *in vitro* properties for [^{18}F]trans-3 and [^{18}F]cis-3, the *in vivo* μPET studies and *ex vivo* data of those radiotracers showed a limited brain uptake and a homogeneous distribution. These preliminary findings speak against the further development of, at least, this class of NR2B NMDAR antagonists as radiotracers for PET imaging. Nevertheless, the *in vivo* studies demonstrated that the radiolabelling position is stable as no defluorination was observed. The 3-[^{18}F]fluoropiperidines could be an advantageous building block to facilitate the development of future radiopharmaceuticals containing a piperidine ring in their structure.

Acknowledgements

This research was supported by the French “Ministère de l’enseignement supérieur et de la recherche” (RK, GG). The authors thank Olivier Tirel and Jérôme Delamare for the cyclotron production of fluorine-18. The authors are grateful to Dr E.T. MacKenzie for the proof reading of this article.

References

- 1 R. Di Fabio, R. Giovannini, B. Bertani, M. Borriello, A. Bozzoli, D. Donati, A. Falchi, D. Ghirlanda, C. P. Leslie, A. Pecunioso, G. Rumboldt and S. Spada, *Bioorg. Med. Chem. Lett.*, 2006, **16**, 1749–1752.
- 2 C. P. Leslie, R. D. Fabio, F. Bonetti, M. Borriello, S. Braggio, G. D. Forno, D. Donati, A. Falchi, D. Ghirlanda, R. Giovannini, F. Pavone, A. Pecunioso, G. Pentassuglia, D. A. Pizzi, G. Rumboldt and L. Stasi, *Bioorg. Med. Chem. Lett.*, 2007, **17**, 1043–1046.
- 3 B. Budzik, V. Garzya, D. Shi, G. Walker, Y. Lauchart, A. J. Lucas, R. A. Rivero, C. J. Langmead, J. Watson, Z. Wu, I. T. Forbes and J. Jin, *Bioorg. Med. Chem. Lett.*, 2010, **20**, 3545–3549.
- 4 M. Morgenthaler, E. Schweizer, A. Hoffmann-Roder, F. Benini, R. E. Martin, G. Jaeschke, B. Wagner, H. Fischer, S. Bendels, D. Zimmerli, J. Schneider, F. Diederich, M. Kansy and K. Muller, *ChemMedChem*, 2007, **2**, 1100–1115.
- 5 Z. Q. Yang, J. C. Barrow, W. D. Shipe, K. A. Schlegel, Y. Shu, F. V. Yang, C. W. Lindsley, K. E. Ritttle, M. G. Bock, G. D. Hartman, V. N. Uebele, C. E. Nuss, S. V. Fox, R. L. Kraus, S. M. Doran, T. M. Connolly, C. Tang, J. E. Ballard, Y. Kuo, E. D. Adarayan, T. Prueksaritanont, M. M. Zrada, M. J. Marino, V. K. Graufelds, A. G. Dilella, I. J. Reynolds, H. M. Vargas, P. B. Bunting, R. F. Woltmann, M. M. Magee, K. S. Koblan and J. J. Renger, *J. Med. Chem.*, 2008, **51**, 6471–6477.
- 6 C. D. Cox, P. J. Coleman, M. J. Breslin, D. B. Whitman, R. M. Garbaccio, M. E. Fraley, C. A. Buser, E. S. Walsh, K. Hamilton, M. D. Schaber, R. B. Lobell, W. Tao, J. P. Davide, R. E. Diehl, M. T. Abrams, V. J. South, H. E. Huber, M. Torrent, T. Prueksaritanont, C. Li, D. E. Slaughter, E. Mahan, C. Fernandez-Metzler, Y. Yan, L. C. Kuo, N. E. Kohl and G. D. Hartman, *J. Med. Chem.*, 2008, **51**, 4239–4252.
- 7 Y. Zhou, K. Vu, Y. Chen, J. Pham, T. Brady, G. Liu, J. Chen, J. Nam, P. S. Murali Mohan Reddy, Q. Au, I. S. Yoon, M. H. Tremblay, G. Yip, C. Cher, B. Zhang, J. R. Barber and S. C. Ng, *Bioorg. Med. Chem. Lett.*, 2009, **19**, 3128–3135.
- 8 A. D. Kerekes, S. J. Esposito, R. J. Doll, J. R. Tagat, T. Yu, Y. Xiao, Y. Zhang, D. B. Prelusky, S. Tevar, K. Gray, G. A. Terracina, S. Lee, J. Jones, M. Liu, A. D. Basso and E. B. Smith, *J. Med. Chem.*, 2011, **54**, 201–210.
- 9 B. Planty, C. Pujol, M. Lamothe, C. Maraval, C. Horn, G. B. Le and M. Perez, *Bioorg. Med. Chem. Lett.*, 2010, **20**, 1735–1739.
- 10 N. J. Liverton, R. A. Bednar, B. Bednar, J. W. Butcher, C. F. Claiborne, D. A. Claremon, M. Cunningham, A. G. Dilella, S. L. Gaul, B. E. Libby, E. A. Lyle, J. J. Lynch, J. A. McCauley, S. D. Mosser, K. T. Nguyen, G. L. Stump, H. Sun, H. Wang, J. Yergey and K. S. Koblan, *J. Med. Chem.*, 2007, **50**, 807–819.
- 11 M. B. van Niel, I. Collins, M. S. Beer, H. B. Broughton, S. K. F. Cheng, S. C. Goodacre, A. Heald, K. L. Locker, A. M. MacLeod, D. Morrison, C. R. Moyes, D. O’Connor, A. Pike, M. Rowley, M. G. N. Russell, B. Sohail, J. A. Stanton, S. Thomas, H. Verrier, A. P. Watt and J. L. Castro, *J. Med. Chem.*, 1999, **42**, 2087–2104.
- 12 R. Schirmacher, B. Wangler and E. Schirmacher, *Mini-Rev. Org. Chem.*, 2007, **4**, 317–329.
- 13 R. Littich and P. J. Scott, *Angew. Chem., Int. Ed. Engl.*, 2012, **51**, 1106–1109.
- 14 P. Paoletti and J. Neyton, *Curr. Opin. Pharmacol.*, 2007, **7**, 39–47.
- 15 C. Beinat, S. Banister, I. Moussa, A. J. Reynolds, C. S. McErlean and M. Kassiou, *Curr. Med. Chem.*, 2010, **17**, 4166–4190.
- 16 J. M. Loftis and A. Janowsky, *Pharmacol. Ther.*, 2003, **97**, 55–85.
- 17 P. L. Chazot, *Curr. Med. Chem.*, 2004, **11**, 389–396.
- 18 F. Sobrio, G. Gilbert, C. Perrio, L. Barré and D. Debruyne, *Mini-Rev. Med. Chem.*, 2010, **10**, 870–886.
- 19 R. Labas, F. Sobrio, Y. Bramoullé, A.-S. Hérard, M. Guillemier, P. Hantraye, F. Dollé and L. Barré, *J. Labelled Compd. Radiopharm.*, 2010, **53**, 63–67.
- 20 R. Labas, G. Gilbert, O. Nicole, M. Dhilly, A. Abbas, O. Tirel, A. Buisson, J. Henry, L. Barré, D. Debruyne and F. Sobrio, *Eur. J. Med. Chem.*, 2011, **46**, 2295–2309.
- 21 R. Koudih, G. Gilbert, M. Dhilly, A. Abbas, L. Barré, D. Debruyne and F. Sobrio, *Eur. J. Med. Chem.*, 2012, **53**, 408–415.
- 22 S. Furegati, W. Ganci, F. Gorla, U. Ringeisen and P. Ruedi, *Helv. Chim. Acta*, 2004, **87**, 2629–2661.
- 23 S. Sonda, T. Kawahara, K. Katayama, N. Sato and K. Asano, *Bioorg. Med. Chem.*, 2005, **13**, 3295–3308.
- 24 S. J. Martin, J. A. Eisenbarth, U. Wagner-Utermann, W. Mier, M. Henze, H. Pritzkow, U. Haberkorn and M. Eisenhut, *Nucl. Med. Biol.*, 2002, **29**, 263–273.
- 25 J. Cossy and D. Gomez Pardo, *Chemtracts: Org. Chem.*, 2002, **15**, 579–605.
- 26 T. X. Métro, B. Duthion, D. Gomez Pardo and J. Cossy, *Chem. Soc. Rev.*, 2010, **39**, 89–102.
- 27 N. J. Liverton, C. F. Claiborne, D. A. Claremon and J. A. McCauley, *WO Pat.*, 2004/108705, 2004.
- 28 C. Addy, C. Assaid, D. Hreniuk, M. Stroh, Y. Xu, W. J. Herring, A. Ellenbogen, H. A. Jinnah, L. Kirby, M. T. Leibowitz, R. M. Stewart, D. Tarsy, J. Tetrad, S. A. Stoch, K. Gottesdiener and J. Wagner, *J. Clin. Pharmacol.*, 2009, **49**, 856–864.